

Observation of a fluctuation-enhanced magnetoresistance in $\text{Ni}_{81}\text{Fe}_{19}/\text{Ag}$ multilayers at high current density

C. T. Rogers, L. S. Kirschenbaum, and P. D. Beale

Condensed Matter Laboratory, Department of Physics, University of Colorado, Boulder, Colorado 80309-0390

S. E. Russek and S. C. Sanders*

Electromagnetic Technology Division, National Institute of Standards and Technology, Boulder, Colorado 80303-3328

(Received 1 August 1997)

We report a correlation between peaks observed in the resistance versus applied magnetic field and low-frequency resistance noise for $\text{Ni}_{81}\text{Fe}_{19}/\text{Ag}$ giant magnetoresistance systems with dc bias current density above 10^6 A/cm². The magnetic noise has a $1/f$ -like spectrum and arises from time-dependent magnetic orientational fluctuations within the multilayer. The noise amplitude is strongly correlated with the observed magnetoresistance peaks. The data and a simple model for the fluctuations demonstrate the important role of fluctuations in determining magnetoresistance in such multilayer systems. [S0163-1829(97)51538-4]

Since the discovery of the giant magnetoresistance (GMR) effect in Fe/Cr multilayers^{1,2} and its extension to magnetic field strengths well below 10 millitesla (mT) for NiFe-alloy/noble metal and Co/noble metal multilayers,³ there has been a growing interest in the physics and application of thin-film multilayer magnetic systems.⁴ A significant theoretical and experimental effort⁵⁻⁹ has resulted in general agreement regarding how the magnetoresistance arises from the underlying magnetic layer orientations: A combination of magnetic interactions (principally magnetostatic, exchange, and Zeeman energies) produce some orientation of magnetic moments in the system. Electron transport senses this magnetic structure via the combination of bulk and surface spin-dependent scattering rates and spin-dependent densities of states. For most thin-film geometries, the magnetic moments are oriented in the plane of the film, with an in-plane angle, θ_j . The magnetoconductivity, i.e., the change in conductivity, $\delta\sigma$, with external field, associated with a given pair of ferromagnetic layers (where spins in each layer are aligned in directions θ_1 and θ_2 , respectively) is found theoretically and experimentally¹⁰ to be such that $\delta\sigma \propto \cos(\theta_1 - \theta_2)$. For small $\delta\sigma$, the magnetoresistance (MR) is similarly found to be $\delta R \propto \cos(\theta_1 - \theta_2)$. For GMR multilayers the magnetoresistance proportionality factor is negative: Higher resistance implies more antiferromagnetic alignment within the multilayer.

It has previously been considered adequate to simplify this description by replacing the angles with their time average values, $\langle \theta_j \rangle$. Most GMR systems appear to be well described by static magnetic configurations, which then influence the electronic resistance. Technological applications of these systems are driving device sizes into the submicrometer region, where such static pictures are bound to fail due to thermal fluctuation effects on moment orientations. In this paper, we present multilayer NiFe/Ag magnetoresistance and resistance noise data that strongly support a picture in which magnetic domain *fluctuations* are an essential element in understanding the MR behavior.

We have described the multilayer film growth and device fabrication in detail elsewhere.¹¹ Briefly, our multilayers are

grown by dc magnetron sputtering. We begin with 300 nm of thermal oxide on a silicon substrate. An initial 10-nm layer of Ta is deposited followed by 2.2 nm of Ag. We then deposit a sequence of either 4, 6, or 8 $\text{Ni}_{81}\text{Fe}_{19}$ (2 nm)/Ag (4.4 nm) bilayers. We complete the structure with a final 2-nm layer of $\text{Ni}_{81}\text{Fe}_{19}$, a 2.2-nm Ag layer, and a 15-nm cap layer of Ta. The finished structure has 5, 7, or 9 ferromagnetic layers buried in a nearly symmetric sequence of Ag and Ta layers. Device structures are patterned using photolithography and Ar ion milling. We have measured the properties of as-grown and annealed¹² multilayers.

We measure the magnetoresistance by biasing the device with a dc current plus a small ac current. The resulting ac voltage is lock-in detected and normalized by the ac current to determine the local resistance. The dc current causes some Joule heating and creates an internal magnetic field that we use along with the external field to produce a magnetic field gradient vertically through the multilayer. We estimate the average current density by the total dc current divided by the device width and total multilayer thickness.

At each point on the MR curve, the resistance noise power spectrum is determined by measuring the voltage fluctuations across the device in the presence of the dc current. We use a commercial spectrum analyzer to determine the voltage power spectral density. Normalization by the square of the dc current then leads to the resistance power spectrum. Measurements take place in a cryostat to allow temperature regulation from 2 to 375 K with a typical stability of 10 mK. Magnetic field was provided by a solenoid with field oriented in the plane of the films and perpendicular to the direction of device current. The maximum field strength was 40 mT.

One of the most striking effects we have previously reported^{13,14} is the observation of multiple peaks in the MR curves for devices under high dc current density bias. Figure 1 shows examples of multi-peaked MR curves for 5-, 7-, and 9-layer devices near 10^7 A/cm² dc bias. The 7-layer sample has been annealed for 5 min. at 350 C in 5% H₂ in Ar. The 5-layer and 9-layer samples are unannealed. Also shown for comparison is the low-current MR curve of the 7-layer sample. In each case, the high-bias behavior shows a se-

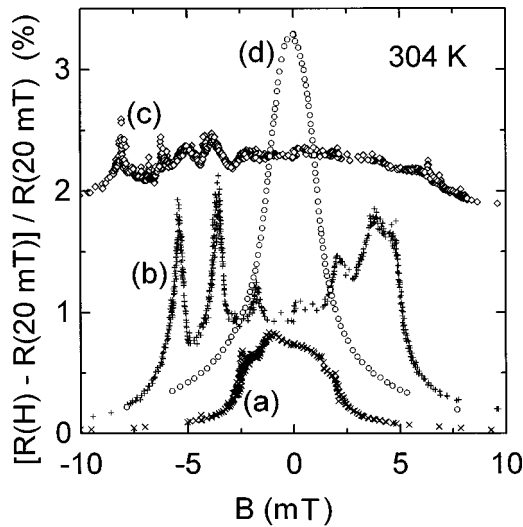


FIG. 1. Magnetoresistance vs external magnetic field for three different NiFe/Ag multilayer devices at 304 K. The figure shows the correlation between the number of magnetoresistance structures and the number of magnetic layers. All devices are nominally $8 \mu\text{m}$ in width. (a) A 5-layer, $32\text{-}\mu\text{m}$ long, unannealed resistor at 40 mA ($1.5 \times 10^7 \text{ A/cm}^2$). $R(20 \text{ mT}) \approx 41.1 \Omega$. (b) A 7-layer, $160\text{-}\mu\text{m}$ long, annealed resistor at 65 mA ($1.8 \times 10^7 \text{ A/cm}^2$). $R(20 \text{ mT}) \approx 64.3 \Omega$. (c) A 9-layer, $32\text{-}\mu\text{m}$ long, annealed resistor at 50 mA ($0.8 \times 10^7 \text{ A/cm}^2$). $R(20 \text{ mT}) \approx 20.7 \Omega$. (d) The 7-layer annealed resistor at zero bias current, $R(20 \text{ mT}) \approx 59.2 \Omega$. The increase in resistance under bias is due largely to Joule heating. Curve (c) has been offset by 1.8% for clarity.

quence of peaks or shoulders. The structures are most apparent on annealed samples, but occur in all cases we have studied. The number of structures is directly correlated with the number of magnetic layers in the device; the peaks occur at external field such that the total local magnetic field on a given magnetic layer, including the dc bias current induced field and magnetostatic field, just balances to zero. At each peak, there is one layer in the film with nearly zero local field, while layers above and below are magnetically saturated in opposite directions.

This balance of local field to near zero strength leaves the balanced layer susceptible to thermal fluctuations and suggests that the MR peaks could be intrinsically due to such fluctuations. To test this hypothesis, we have investigated the resistance fluctuations to see if the MR peaks are correlated with increased noise. For all NiFe/Ag devices we have studied, at all temperatures and current densities where magnetoresistance peaks are observed, we find a strong correlation between MR and noise. We find that the noise is described by a $1/f$ -like spectrum with smooth frequency and field-dependent structure. At each peak in the MR curve, we find a significant increase in the noise spectral density over the entire experimentally measured frequency band (0.1 Hz to 10 kHz). The noise near the resistance peaks can be nearly two orders of magnitude larger than that found away from the peaks. In Fig. 2, we show MR and resistance noise power spectral density at 1 Hz over the full magnetic field range for a 7-layer, $16\text{-}\mu\text{m}$ wide device with an average dc current density of $8 \times 10^6 \text{ A/cm}^2$. In Fig. 3, we show a sequence of resistance noise power spectra, versus frequency and external magnetic field in the region of the MR peak at -2.5 mT .

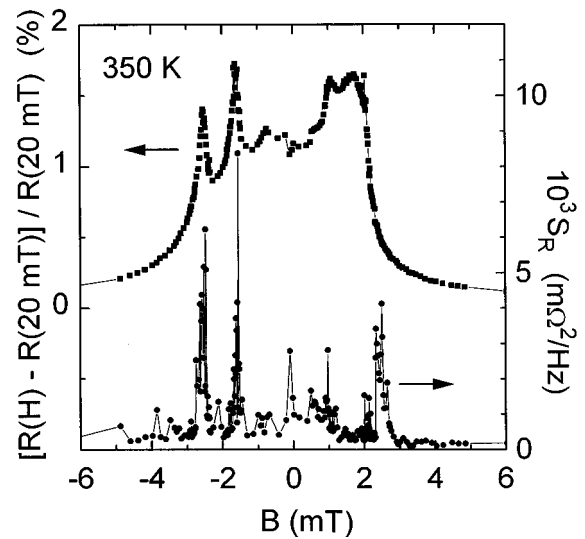


FIG. 2. Plot of magnetoresistance and resistance noise power spectral density at 1 Hz for a 7-layer, $16\text{-}\mu\text{m}$ wide, $160\text{-}\mu\text{m}$ long device at $0.8 \times 10^7 \text{ A/cm}^2$ and at 350 K. $R(20 \text{ mT}) \approx 30.9 \Omega$. The plot shows the strong correlation between regions of high noise and peaks in the magnetoresistance.

These observations provide insight into the magnetic orientation behavior that leads to the observed MR peaks. First, we consider the observed $1/f$ -like spectrum: It is known¹⁵ that resistance fluctuations from individual magnetic domains can be observed in the low-frequency resistance noise of small NiFe/Ag multilayer structures. For micrometer-sized devices, single domain reorientations result in discrete changes in device resistance on the order of 1 mΩ. Magnetic field dependence of the switching suggests a typical domain

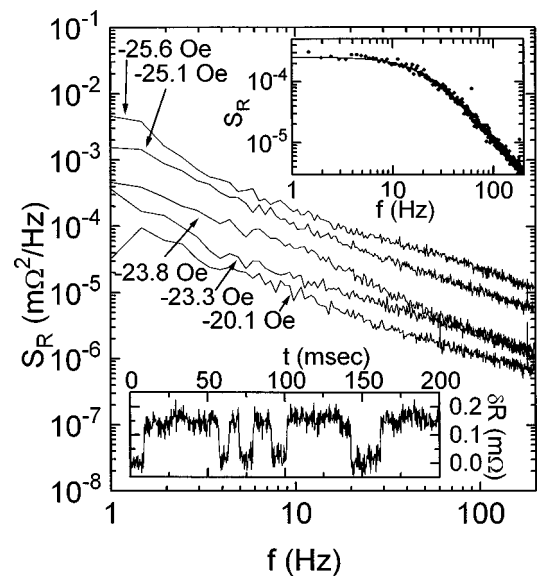


FIG. 3. Family of curves showing the low-frequency resistance noise power spectrum, $S_R(f)$, at several different external magnetic fields for the device of Fig. 2 in the region of the left-most MR peak. Lower left inset shows characteristic two-level switching behavior of the resistance as described in the text, while upper right inset shows the Lorentzian power spectrum associated with the two-level switching. The observed $1/f$ -like spectrum is a combination of many active two-level switching systems.

moment of $\sim 10^6 \mu_B$, where μ_B is the Bohr magneton. This type of two-level “switching” noise leads to Lorentzian contributions to the resistance power spectrum. Similar switching noise is observed in our larger devices, with switching amplitudes near $100 \mu\Omega$ for $16 \mu\text{m}$ device widths. Such resistance switching for the $16\text{-}\mu\text{m}$ wide device of Figs. 2 and 3 and the associated Lorentzian power spectrum is shown in the insets to Fig. 3 (data is taken at $+3 \text{ mT}$, away from large noise peaks). The larger number of domains active in a given bandwidth in a large device makes it less likely that only a single domain will be isolated in the power spectrum. Thus, for larger devices, we typically see time records in which multiple switchers are visible. The collection of Lorentzian spectra overlap to form the observed $1/f$ -like spectra as in Fig. 3.

The observed large increase in the ensemble $1/f$ -like noise thus apparently arises from an increase in the number of fluctuating domains in the region of the MR peaks. This hypothesis is consistent with our picture of the local magnetic environment: Near each MR peak, the local field strength on the balanced layer is small and the typical magnetic domain in the layer is most susceptible to thermally driven reorientations. The correlation that we observed between the MR peaks and resistance noise strongly suggests that the peaks arise from magnetic domain orientation fluctuations.

To further elucidate the role of fluctuations in this system, we have investigated a theoretical model based on the work of Camley and Stamps.⁵ Each magnetic layer in Camley’s model is described by a single classical spin. For N layers with only nearest-neighbor interactions, the system is described by an energy function with magnetostatic exchange-like terms and Zeeman terms for each layer:

$$E(\theta_j) = \sum_{j=1}^{N-1} J_{\perp} \cos(\theta_j - \theta_{j+1}) - \sum_{j=1}^N m_j \mu_0 H_j \cos(\theta_j). \quad (1)$$

Here, J_{\perp} is the interaction strength between neighboring layers, due to local magnetostatic interactions.¹⁶ The angles, θ_j , are measured between the external field direction and the layer moment. Smith¹⁷ has shown that the local field, H_j , is a superposition of the external applied field, H_{ext} , fields due to internal magnetostatics, H_M , and the field arising from the dc bias current, $H_j \approx Jz/2$, where J is the current density and z is the distance of the layer from the multilayer midplane. Finally, m_j is the strength of the layer magnetic moment, and μ_0 is the permeability of free space. This model accurately associates the peak positions with the external field necessary to produce zero local field at a given layer.¹³

In Camley’s picture, m_j is assumed to be representative of the moment of an entire magnetic layer in the film. However, in $\text{Ni}_{81}\text{Fe}_{19}/\text{Ag}$ annealed multilayer, diffusion of Ag into grain boundaries in the magnetic layers leads to a weakening of the grain-to-grain in-plane magnetostatic coupling strength, J_{\parallel} , relative to J_{\perp} .¹² Thus, an N -layer system can be thought of as being composed of microscopic columnar regions, characterized by the grain size, within which there are N magnetic “pancakes” that interact with the neighbors above and below with strength J_{\perp} and interact with surrounding pancakes within the same layer with a weaker J_{\parallel} .

As a first approximation we ignore J_{\parallel} . Equation (1) then describes the energy of a microscopic stack, where m_j and J_{\perp} are now representative of single magnetic pancakes. For simplicity, we assume that the pancakes all have the same moment amplitude so that $m_j = m$. The complete multilayer is then modeled as a noninteracting ensemble of such stacks or domains. The magnetoresistance is related to the quantity, $\cos \delta\theta \equiv \sum_{j=1}^{N-1} \cos(\theta_j - \theta_{j+1})$. Equation (1) is used in a statistical calculation to generate the mean value, $\langle \cos \delta\theta \rangle$, and its variance $\langle (\cos \delta\theta)^2 \rangle - \langle \cos \delta\theta \rangle^2$, i.e., quantities, respectively, related to the average MR and its fluctuations.

In certain regimes the partition function for this model can be calculated analytically. The mean value and variance are then determined via partial derivatives of the partition function with respect to J_{\perp} . For an N -layer system at high internal bias and modest temperature, we find that both quantities can be derived in terms of the n th order modified Bessel functions, $I_n(x)$.¹⁸ We define three dimensionless functions, $\Omega(x) \equiv I_1(x)/I_0(x)$, $\Phi(x) \equiv \Omega(x)/x$, and $\Psi(x) \equiv \frac{1}{2}[1 + I_2(x)/I_0(x)] - \Omega^2(x)$ in terms of which the mean and variance can be written as

$$(N-1) - \langle \cos \delta\theta \rangle \approx \Omega \left(\frac{mB_{\text{ext}} + \frac{N-1}{2} mB_1 + J_{\perp}}{k_B T} \right) - \Omega \left(\frac{mB_{\text{ext}} - \frac{N-1}{2} mB_1 - J_{\perp}}{k_B T} \right) + \frac{2J_{\perp}}{mB_1} \sum_{j=1}^{N-2} \Phi \left(\frac{mB_{\text{ext}} - \left(j - \frac{N-1}{2} \right) mB_1}{k_B T} \right), \quad (2)$$

$$\langle \cos \delta\theta^2 \rangle - \langle \cos \delta\theta \rangle^2 \approx \Psi \left(\frac{mB_{\text{ext}} + \frac{N-1}{2} mB_1 + J_{\perp}}{k_B T} \right) + \Psi \left(\frac{mB_{\text{ext}} - \frac{N-1}{2} mB_1 - J_{\perp}}{k_B T} \right) + \frac{2k_B T}{mB_1} \sum_{j=1}^{N-2} \Phi \left(\frac{mB_{\text{ext}} - \left(j - \frac{N-1}{2} \right) mB_1}{k_B T} \right), \quad (3)$$

where $B_1 = \mu_0 H_1$ is the increment of current-induced magnetic induction from one layer to its neighbor. These results are valid for $mB_1 \gg J_{\perp}$ and in the temperature range $J_{\perp} \gg k_B T \gg J_{\perp}(J_{\perp}/mB_1)$. These conditions hold for the data presented here.

In both expressions, the first pair of terms describe the behavior of the outer-most magnetic layers, while the summation terms represent essentially identical behavior for the internal magnetic layers. Figure 4 shows plots of these func-

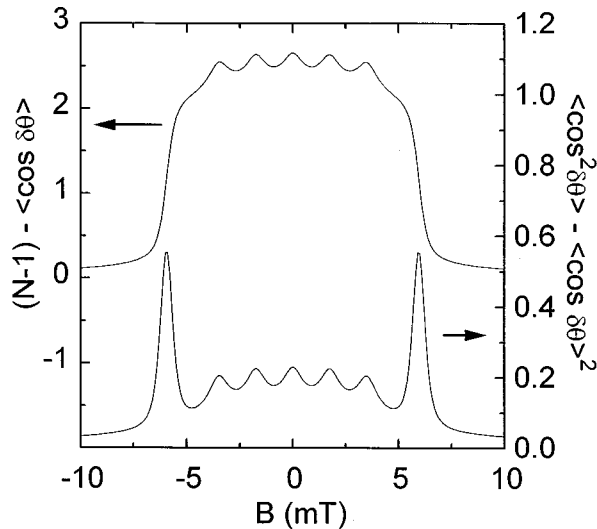


FIG. 4. Approximate analytic results, Eqs. (2) and (3), for $(N-1) - \langle \cos \delta \theta \rangle$ (the theory equivalent of the magnetoresistance) and its variance for a 7-layer system with $mB_{\perp}/J_{\perp} = 2.5$ and $k_B T/J_{\perp} = 0.3$, roughly the conditions realized experimentally in the case of the 7-layer sample in Fig. 1(b), (assumes that $m = 2 \times 10^6 \mu_B$). Monte Carlo results obtained for Eq. (1) are nearly indistinguishable from the solid lines.

tions versus external field for a 7-layer system, with conditions that approximate those found experimentally in Fig. 1 and assuming $m = 2 \times 10^6 \mu_B$. For magnetic layers internal to the multilayer, we find peaks in both quantities at positions in good agreement with the observations. The major discrepancy between the model and the data appears to be the lack of calculated MR peaks at the outside layer positions. A variety of modifications of the model, including reintroduction of the J_{\parallel} terms,¹⁸ predict MR peaks at these edge positions. However, the simple model provides a good qualitative description of the magnetoresistance and noise.

The model traces the magnetoresistance peaks and associated noise peaks to fluctuations in the relative domain orientations. Consider the layer with weak local field: The layers above and below feel relatively strong local fields and are roughly saturated in opposite directions. According to the expected $\sum \cos \delta \theta_j$ dependence for magnetoresistance, a single layer free to rotate between fixed layers oriented 180° apart causes *no* change in magnetoresistance. However, when the neighboring layers are allowed to react to fluctuations in the central layer orientation, they respond by orientational motion in an effort to minimize their local energy. This response causes an increase in antiferromagnetic alignment between themselves and their neighbors. The increased antiferromagnetic order leads on average to the observed magnetoresistance peaks, coincident with the maximum noise. The MR peaks are a fluctuation enhanced magnetoresistance.

This behavior at high current densities differs significantly from that observed for low-current density NiFe/Ag or Co/Cu GMR systems,^{19,20} and can be traced largely to the effect of the internal bias field. The recent noise measurements of Smith *et al.* on high-current density biased NiFe/Cu and NiFeCo/Cu multilayers²¹ bear some resemblance to our results (though discrete peaks were not resolved), suggesting that the picture that we have developed for the MR and associated noise in high-current density biased NiFe/Ag multilayers likely applies more generally. Our results demonstrate the importance of including the fluctuation effects in the complete description of GMR. Such effects are likely to become more pronounced and important as device dimensions and characteristic domain magnetic moments are reduced in size.

We gratefully acknowledge helpful discussions with Leo Radzihovsky. L.S.K. acknowledges support from the National Institute of Standards and Technology PREP Program. S.E.R. and S.C.S. acknowledge support from the NIST Advanced Technology Program.

*Present address: Quantum Peripherals Colorado, Inc. 2270 S. 88th St. Louisville, CO 80028-8188.

¹M. N. Babich, J. M. Broto, A. Fret, F. Nguyen Van Dau, F. Petroff, P. Eitenne, G. Creuzet, A. Feiderich, and J. Chazelas, *Phys. Rev. Lett.* **61**, 2472 (1988).

²G. Binasch, P. Runberg, F. Saurenbach, and W. Zinn, *Phys. Rev. B* **39**, 4828 (1989).

³B. Dieny, V. S. Speriosu, and S. S. P. Parkin, *Phys. Rev. B* **43**, 1297 (1991).

⁴See, for example, *Proceedings of the 1995 Intermag. Conference* [IEEE Trans. Magn. **31** (1995)], pp. 4080–4198.

⁵R. E. Camley and R. L. Stamps, *J. Phys. Condens. Matter* **5**, 3727 (1993), and references therein.

⁶R. E. Camley and J. Barnas, *Phys. Rev. Lett.* **63**, 664 (1989).

⁷P. M. Levy, S. Zhang, and A. Fert, *Phys. Rev. Lett.* **65**, 1643 (1990).

⁸Randolph Q. Hood and L. M. Falicov, *Phys. Rev. B* **46**, 8287 (1992).

⁹H. E. Camblong, P. M. Levy, and S. Zhang, *Phys. Rev. B* **51**, 16 052 (1995).

¹⁰A. Chaiken, G. A. Prinz, and J. J. Krebs, *J. Appl. Phys.* **67**, 4892

(1990).

¹¹Y. K. Kim and S. C. Sanders, *Appl. Phys. Lett.* **66**, 1009 (1995).

¹²T. L. Hylton, K. R. Coffey, M. A. Parker, and J. K. Howard, *Science* **261**, 1021 (1993).

¹³L. S. Kirschenbaum, C. T. Rogers, P. D. Beale, S. E. Russek, and S. C. Sanders, *Appl. Phys. Lett.* **68**, 3099 (1996).

¹⁴L. S. Kirschenbaum, C. T. Rogers, P. D. Beale, S. E. Russek, and S. C. Sanders, *IEEE Trans. Magn.* **32**, 4684 (1996).

¹⁵L. S. Kirschenbaum, C. T. Rogers, P. D. Beale, S. E. Russek, and S. C. Sanders, *IEEE Trans. Magn.* **31**, 3943 (1995).

¹⁶J. C. Slonczewski, *J. Magn. Magn. Mater.* **129**, L123 (1994).

¹⁷Neil Smith, *IEEE Trans. Magn.* **30**, 3822 (1994).

¹⁸P. D. Beale, Leo Radzihovsky, and C. T. Rogers (unpublished).

¹⁹Michael A. Parker, Kevin R. Coffey, J. Kent Howard, Ching H. Tsang, Robert E. Fontana, and Todd L. Hylton, *IEEE Trans. Magn.* **32**, 142 (1996).

²⁰H. T. Hardner, M. B. Wiessman, and S. S. P. Parkin, *Appl. Phys. Lett.* **67**, 1938 (1995).

²¹Neil Smith, Alexander M. Zeltser, and Martin R. Parker, *IEEE Trans. Magn.* **32**, 135 (1996).